CAVITATION DURING TENSILE DEFORMATION OF ISOTHERMALLY CRYSTALLIZED POLYPROPYLENE AND HIGH DENSITY POLYETHYLENE

Andrzej Pawlak

Centre of Molecular and Macromolecular Studies, Polish Academy of Sciences, Sienkiewicza 112, 90-363 Lodz, Poland

Corresponding author: apawlak@cbmm.lodz.pl, phone 48 42 6803223, fax 48 42 6847126

Keywords: polypropylene, polyethylene, cavitation, tensile properties, plastic deformation, isothermal crystallization.

ABSTRACT

The cavitation phenomenon was studied in isothermally and non-isothermally crystallized polypropylene and high-density polyethylene. I found that nano-voids were not present in the crystallized samples, but were formed during their tensile deformation. The process of cavitation was initiated before reaching the yield point. The ellipsoidal voids were initially elongated perpendicularly to the deformation direction, but if the polymer (i.e. HDPE) was able to deform beyond the yield then reorientation of voids into the deformation direction was observed at local strains of 100-200 % . This behaviour was similar to that observed previously in the samples crystallized without an exact control of solidification conditions. The calculations of Guinier's radius showed that voids in deformed PP samples, were characterized by the gyration radii of 28-50 nm. Smaller voids were observed in polyethylene. The scale of cavitation during deformation, studied on the example of polyethylene, depended on the preceding crystallization process and was most intensive for the specimens crystallized at the highest temperature of 125°C.

INTRODUCTION

The cavitation phenomenon was discovered in many semicrystalline polymers. The generation of voids (cavities) is usually observed in two different circumstances: during isothermal crystallization [1-9] and during tensile deformation [10-14]. To my knowledge, so far both cases have been analyzed and described separately. The reason of cavitation during isothermal crystallization is the existence of pockets of melt surrounded by growing spherulites. The volume of molten material in these pockets (called weak spots) is not sufficient for complete crystallization because the density of crystalline phase is higher than the density of molten polymer [2]. The negative (i.e. 3D tensile) pressure arises inside the weak spot with time and as a result the growth of neighbour spherulites becomes slower and the polymer melt is stretched. Estimations show that the negative pressure in polypropylene (PP) weak spots may be high, even 19-40 MPa [1,3].

When the negative pressure reaches the level of cohesive strength of melt then a rapid break of melt occurs and one- or more micrometer voids are formed. The presence of a cavitation nucleus (e.g. impurities) supports initiation of the process at lower pressure. Often the fracture of melt is observed at the same time in adjacent weak spots, which suggests that the propagation of an acoustic wave emitted in the cavitation act, resulting from a sudden pressure change, induces the cavitation in other weak spots. The acoustic emission from crystallizing polymer was recorded by Galeski et al. [4]. Cavitation relaxes stresses inside the weak spot and the growth rate of spherulite increases to the initial level [1].

If the pocket of melt occluded by spherulites is small, the negative pressure may be insufficient for rupture of the structure and the material solidifies without break, but with frozen internal stresses. Nowacki et al. [5] reported that the large weak spots tended to cavitate at lower negative pressure than smaller ones, which resulted from an increased probability of the presence of a cavitation nucleus inside the confined melt. It was also found that the shape of cavities in polypropylene depended on the temperature of crystallization – at low temperatures the voids were

spherical, at high temperatures (i.e. >135°C) the voids were elongated (similar to cracks), formed along interspherulitic boundaries [5, 6]. Voiding in weak spots was not observed in thin films of polymers crystallized with a free surface, because the deficiency of crystallizing material was compensated here by thinning of the film. The cavitation during crystallization usually did not occur when the process was non-isothermal, because the spherulites were small, a typical size of weak spots was also small, the time of crystallization was short and the value of negative pressure was below the limit of melt strength.

The above discussed experiments were focused on the studies of cavitation in thin films of crystallizing polymers [5-9]. Galeski and Piorkowska examined volume samples of polypropylene which were crystallized isothermally at 125°C [2]. They confirmed the existence of weak spots by means of infrared microscopy and the relaxation of stresses after cavitation using Raman spectroscopy. In the second experiment, with the same polymer crystallized in non-isothermal conditions, the authors observed formation of large, 1-2 mm cavities, when the temperature inside the thick specimen decreased much slower than the temperature of skin layer. Similar conditions often exist in the central parts of injected PP shapes, where –if the time of solidification is long enough – large cavities visible even by the naked eye are formed. The pressure inside these cavities, detected by glow discharge from residual gases under high frequency electromagnetic field, was less than 0.1 kPa (i.e. less than 0.1% of atmospheric pressure) [2].

It is known that non-isothermally crystallized semicrystalline polymers can cavitate during deformation [10, 11]. This happens only in tensile mode, never during compression. Usually prime voids are generated around the yield point [12, 13]. We showed that there is a competition between two processes possible at yield in the semicrystalline polymer: plastic deformation of crystals by chains slip mechanism and breaking of amorphous phase (cavitation) [10]. If the polymer crystals are defected, including many dislocations, then with an increase of force the initiation of plastic deformation of lamellae is more probable than the break of amorphous phase. The phenomenon of cavitation in such a polymer is not observed. If lamellae in the polymer are thick, with a reduced

number of defects then the strength of amorphous phase is lower than the stress initiating plastic deformation of crystals and cavitation occurs. It was shown that the same kind of polymer, depending on crystallization and testing conditions (i.e. strain rate, temperature), might cavitate or not [13, 14].

The voids, if present, play an important role during plastic deformation of semicrystalline polymers. The rapid change of local stress due to voids formation stimulates the deformation processes in surroundings crystals, making the deformation of crystals easier. It is visible as a decrease of yield stress, more intensive fragmentation of lamellae and increase of heat generated in the cavitating polymer, when compared with the same kind of material which does not cavitate [10, 15].

Usually, the studies of isothermal crystallization are performed on small pieces of thin polymeric films and this is a reason why information about the mechanical properties of polymers crystallized by this way is limited. The ductile-brittle transition of isotactic polypropylene and its blend with poly(ethylene-co-octene), controlled by isothermal crystallization, was studied by Pang et al. [16]. The mechanical properties of samples, crystallized at 130°C, were poor with breaking at strain of 9%, immediately after the yield. Cavities were not visible in non-deformed samples.

Some studies of the mechanical properties of isothermally crystallized linear polyethylene were performed by Kennedy et al. [17] who analyzed the influence of molecular weight on tensile properties and brittle-ductile transition. The narrow fractions of polyethylenes with molecular mass below 10^5 g/mol were brittle when crystallized at 125-130°C, but showed transitional properties when their molecular mass was larger. Crystallinity was usually high, e.g. 91% for polyethylene with $M_w=1.39*10^5$ g/mol, crystallized at 125 or 130°C.

To my knowledge, there was no report on studies on cavitation during tensile deformation of polymers crystallized isothermally, containing some micrometer size cavities due to crystallization process. It is not even known if nano-voids accompany micro-voids in an isothermally crystallized polymer. The main subject of this work was to observe nano-cavitation during deformation in

isothermally and non-isothermally crystallized polyolefins: high-density polyethylene and polypropylene.

EXPERIMENTAL

MATERIALS AND METHODS

Polypropylene used in these studies was Malen P, F401 (M_w=297200 g/mol, M_n=56400 g/mol, MFR 3g/10 min (at 190°C, 2.16 kg)), produced by Basell Orlen Polyolefins. The second polymer, high-density polyethylene (HDPE) Lupolen 6021D (M_w=1.8*10^5 g/mol, M_w/M_n=7.2), was produced by BASF. Isothermal crystallization process and crystallinity of materials were studied by differential scanning calorimetry (DSC). Thermal Analysis TA 2000 apparatus was used to determine the total time of crystallization. Polymers for DSC studies were formed into 0.5 mm thick films by using a hot laboratory press. Pieces weighing 8-9 mg were cut from these films, encapsulated and crystallized isothermally in the DSC apparatus after melting.

The crystallization of polypropylene was performed at the temperatures of 125, 129, 133 and 137°C. The aim of measurements was to determine crystallization time adequate for samples dedicated to studies of mechanical properties. Dependences of heat flow on time for PP samples are shown in Fig. 1. It was observed that in each case the crystallization process was finished after some time increasing with the temperature of crystallization. Table 1 shows the times and temperatures which were selected as appropriate for the crystallization of samples designed for future studies.

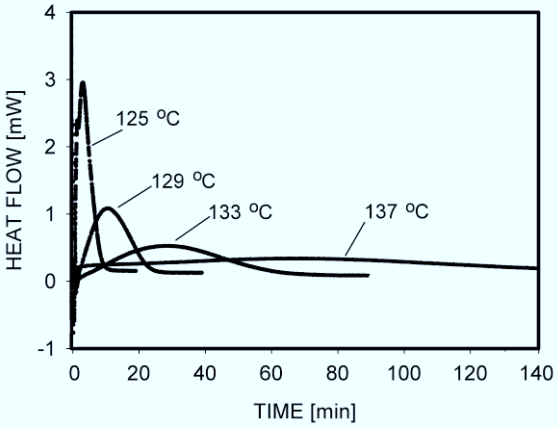


Fig. 1 Heat flow as a function of time during isothermal crystallization of PP samples at selected temperatures: 125, 129, 133 and 137°C

Table 1. Times of crystallization determined from DSC studies as appropriate for the crystallization of samples designed for mechanical studies.

Polypropylene		High Density Polyethylene	
Crystallization temperature [^{o}C]	Time of crystallization [min]	Crystallization temperature [^{o}C]	Time of crystallization [min]
125	20	122	15
129	30	125	30
133	60	129	>90
137	100		

The DSC apparatus was also used to determine crystallization times for high-density polyethylene. The studies were done at crystallization temperatures of 122, 125 and 129°C. The crystallization times selected for preparation of HDPE samples designed for mechanical tests are shown in Table 1. The crystallization process was very slow for a sample remaining at 129°C, so I concluded that this temperature was too high for sample preparation, because there was a risk of thermal degradation.

The DSC technique was used to determine the melting temperature, crystallinity and mean

lamellae thickness of polypropylene. The measurements were done when the samples were heated at the rate of 10 K/min. The heat of melting equal 165 J/g [7] for polypropylene was assumed in the calculations of crystallinity degree. The mean thickness of lamellae, L_m, was determined from Equation 1:

$$L_m=2*\sigma_e*T_{mo}/(H_f*\rho_c*(T_{mo}-T_m)) \quad (1)$$

where σ_e is the surface energy, T_{mo} – equilibrium melting temperature, H_f – heat of fusion, ρ_c – density of crystalline phase, T_m – temperature of melting. The following values were taken for calculations: $\sigma_e=62.3*10^{-7}$ J/cm^2, $T_{mo}=208$°C [7], $H_f=165$ J/g [7], $\rho_c=0.936$ g/cm^3. Similar calculations were done for high density polyethylene specimens, assuming the heat of fusion per unit volume $\Delta H_f=H_f*\rho_c= 280$ J/cm^3 [18], $\sigma_e=4.4*10^{-6}$ J/cm^2 [19], $T_{mo}=415$ K [19].

Samples for a mechanical test were prepared using a hot stage constructed in my laboratory. The main elements of the hot stage were two copper blocks, containing heaters. The heaters and thermometers (resistors) were placed inside the blocks whose temperature was controlled by two programmable 535 Process Controllers (Omega, USA). A thin (0.5 mm) film of polymer was placed between two microscopic glasses and such a sandwich was positioned between the heating blocks. The hot stage with the sample was fixed in a polarizing microscope, replacing an original microscopic stage. Two small holes drilled inside the blocks gave a possibility to observe the growth of crystalline structures inside the examined film. The polypropylene film was heated at the rate of 10°C/min to the temperature of 220°C, kept 3 min at that temperature and cooled down to the final crystallization temperature, again at the rate of 10°C/min. The crystallization temperature for polypropylene was 125, 129, 133 or 137°C. The growth of spherulites was observed during solidification and it was concluded that the images were invariable after times of 20, 30, 60 and 100 min, so after these times the samples were cooled to room temperature. The above-mentioned times of crystallization were the same as determined by DSC (Fig. 1).

Some PP samples were also crystallized non-isothermally, with the aim to compare the properties of differently prepared materials. In this case the polypropylene film was melted at

220°C and after 3 minutes of conditioning the temperature of stage was linearly decreased to 25°C, with the cooling rate of 5°C/min. This rate ensured that the crystallization process was not very fast and the polypropylenes having relatively large and not much defected lamellae should be able to cavitate during deformation. Table 2 presents a list of isothermally crystallized PP samples prepared for mechanical studies.

Table 2. List of samples studied in mechanical and SAXS tests.

Sample name	Polymer	Crystallization conditions
PP-N	Polypropylene	Non isothermal, melting at 220°C, 3 min and cooling 5°C/min
PP 125		Isothermal, 125°C, 20 min
PP 129		Isothermal, 129°C, 30 min
PP 133		Isothermal, 133°C, 60 min
PP 137		Isothermal, 137°C, 100 min
PE-N	High density polyethylene	Non isothermal, melting at 190°C, 2 min and cooling 4°C/min
PE 122		Isothermal, 122°C, 25 min
PE 125		Isothermal, 125°C, 40 min

High-density polyethylene films were prepared similarly to PP films. The 0.5 mm thick foils, formed by the hot press, were melted inside the heating stage, conditioned for 2 min at T=190°C and cooled down at the rate of 10°C/min to one of crystallization temperatures: 122 or 125°C. At these temperatures the film was kept for 25 or 40 min, respectively. The structures growing in polyethylene were small, the evolution of morphology poorly visible with the microscope and the end of crystallization difficult to determine. This was the reason why the crystallization times were a bit longer than recommended by the DSC observations (see Table 1), remembering that the DSC measurements were done in similar, but not exactly the same conditions. Moreover, the longer time should result in the thickening of crystals, which would increase a possibility of cavitation.

Part of polyethylene samples was also crystallized in non-isothermal conditions. In this case

the polymer film was melted inside the crystallizing device at 190°C and after 2 minutes of conditioning at this temperature the samples were cooled down at the rate of 4°C/min to the final temperature of 100°C. Microscopic observations confirmed that the crystallization was finished before reaching the final temperature, so the film was next cooled down to room temperature and removed from the apparatus.

It is known that the process of isothermal crystallization examined in the microscale depends on temperature. For PP and HDPE three crystallization regimes are distinguished and the architecture of solidified polymers depends on these regimes [7,20,21]. All studied here polypropylene samples were crystallized in regime III and HDPE samples were crystallized in regime II.

Samples for the tensile test were cut from the above mentioned films. They had a dog-bone shape, with initial gauge zone length of 12.5 mm, width of 4.1 mm and thickness of 0.3-0.5 mm (PP) or 0.5-0.6 mm (HDPE). Table 2 describes symbols used in the text and the crystallization procedures for polymer samples examined by the tensile test and by X-ray scattering measurements.

Mechanical properties of polymers were studied at room temperature using an Instron 5582 tensile machine. Five samples of each kind were tested in uniaxial drawing. The rate of deformation was 5%/min (i.e. $8.3*10^{-4}$ s^{-1}) for HDPE and 2%/min (i.e. $3.3*10^{-4}$ s^{-1}) for PP. Black marks were drawn on the surface of each specimen. Changes of initial 1 mm distances between the marks were recorded using a Canon D50 digital photo camera. At the same time the actual sample width was recorded. My samples were too thin for accurate measurements of thickness by the photo method, so it was assumed that the thickness changed proportionally to the changes of width.

The local strain of a sample, ε, was determined from Eq. 2:

$$\varepsilon = [(L-L_o)/L_o]*100 \quad [\%] \qquad (2)$$

where L_o=1 mm is the initial distance between black marks, L – distance between marks in the deformed sample. Similarly, volume strain, ΔV, may be defined as:

$$\Delta V = (V-V_o)/V_o, \qquad (3)$$

where V_o is the initial volume and V is the actual volume. Both these volumes were calculated from the width of sample, its thickness (assumed proportional to the width) and distance between black marks, all measured for the most deformed part of the sample. The proportionality of width and thickness changes was controlled for selected strains.

Some mechanical experiments were performed using a laboratory tensile machine, constructed in the Hasylab laboratory in Hamburg. The technical characteristic of this device was similar to Instron, but with the applied force limited to 100 N. This machine was movable, so it was possible to place the stretched sample on the way of X-ray beam from DORIS III synchrotron source (A2 beamline) and conduct X-ray scattering measurements *in situ* during deformation. Radiation, with the wavelength of 0.15 nm, scattered under small angles (SAXS) was detected by a MarCCD two-dimensional detector. SAXS patterns were later used to detect cavities and to determine crystalline structure parameters. It was possible to detect nano-cavities with dimensions below 80 nm. The time of a single pattern registration was 24 s for PP and 6 s for HDPE. The CCTV camera connected to a monitor and computer helped in observation and recording of distances between the marks on specimen surface and in observation of the X-ray beam position on this surface. Before deformation the beam was positioned in place where the beginning of plastic deformation could be expected. If the neck was formed in the expected illuminated area then results of the test were analyzed. The examined PP samples were deformed to break, which happened quickly after the yield point. Mechanical tests of HDPE specimens were stopped at the engineering strains of 90-110%, because in this polymer the most interesting phenomena occur earlier, around the yield point.

On the SAXS pattern representing the scattering from non- deformed semicrystalline polymer only one maximum of intensity, resulting from the crystalline periodic structure, is usually visible. This maximum was used to determine a long period of structure based on the dependence of $Is^2=f(s)$, where I is the intensity and s is the scattering vector [22]. For comparison, the long periods were also determined by a correlation function method [23-24]. With this method the contributions

from amorphous and crystalline phase were separated and their thickness were calculated. The evidence of cavitation process, when examined by SAXS, is a large increase of the scattering intensity. When the concentration of cavities is small and they are dispersed in the polymer matrix, the radius of gyration R can be determined from the equation:

$$I(s) = I_o \rho^2 v^2 \exp(-4\pi^2 s^2 R^2/3) \quad (4)$$

where I –intensity of scattering, I_o – initial intensity of beam, ρ – difference of electron density between the void and matrix, v –volume of scattering objects, s – scattering vector, R – gyration radius [25]. If the scattering objects are randomly oriented then the radius does not depend on the direction of measurement and may be used for determination of the size of cavities if their shape is known. Otherwise, R depends on the direction and only rough information about voids size is provided.

The wide angle X-ray scattering (WAXS) camera was used for observations of possible crystallographic transformations. A source of CuK_α radiation, operating at 30 kV and 50 mA was used. Two-dimensional scattering images were recorded by a camera equipped with a Kodak imaging plate. The distance between a sample and recording plate was 5 cm. Exposed imaging plates were analyzed with PhosphorImager SI system (Molecular Dynamics). The stretching of samples was interrupted at selected strain and the sample was fixed in a special frame, which preserved state of strain. The frame with sample was then placed in a holder of WAXS apparatus. Typical time of acquisition was 7 min. For some samples WAXS patterns were recorded after releasing the mechanical stress with the aim of detection of eventual changes of diffraction patterns.

The spherulitic morphology of polypropylene was studied using the polarized light microscope. Thin, 20 μm, slices were cut from polymer films with a microtome equipped with a glass knife. This procedure was not applied for polyethylene, because the expected size of spherulites (based on crystallization observation) was too small for exact microscopy observations.

RESULTS AND DISCUSSION

a) **Polypropylene**

The crystalline structures of polypropylene films, crystallized according to the procedures described in Table 2, were determined by the DSC and SAXS methods and observed by polarized light microscopy. The long period of lamellar structure was calculated both from the maximum on SAXS intensity curve and from correlation function. The latter method gives also information about the thickness of crystalline and amorphous components. Results of SAXS experiments are collected in Table 3.

Table 3 shows that long period of polypropylene structure depends on the crystallization temperature. It was the smallest (15.6 nm) for non-isothermally crystallized PP and increased with isothermal crystallization temperature to 20.7 nm at T=137°C. A similar tendency was observed when the long period was calculated from correlation function. In all examined materials crystalline layers were thicker than amorphous ones and lamellae thickness increased with crystallization temperature.

Table 3. Results of SAXS and DSC experiments for non-deformed PP samples.

Temperature of crystalli-zation [°C]	SAXS			DSC			
	Long period from intensity curve [nm]	Long period determined from correlation function [nm]	Lamellae thickness determined from correlation function [nm]	Temperature of melting, max [°C]	Lamellae thickness [nm]	Heat of melting [J/g]	Crystallinity [%]
Non isothermal	15.6	14.6	9.3	165.3	9.1	108	65
125	17.6	16.7	11.3	164.4	8.9	115	69

129	19.1	18.5	11.8	165.3	9.1	117	71
133	19.7	18.1	12.4	166.9	9.4	120	73
137	20.7	18.6	12.0	168.2	9.8	121	73

The second source of information on the crystalline structure of polypropylene was the DSC technique. Results of these studies are also presented in Table 3, where the following parameters are shown: temperature of melting (maximum of peak), lamellae thickness, heat of melting and crystallinity.

DSC thermogram of non-isothermally crystallized PP sample shows that the melting peak was wide, with a maximum at 165.3°C. Melting peaks in the isothermally crystallized specimens were narrower. The shift of position of the maximum in the direction of higher temperature was observed with the increase of crystallization temperature. Calculations of the lamellae thickness (Eq. 1) showed its increase with the crystallization temperature. It follows from Table 3 that the heat of melting is higher at higher temperatures, which means an increase of crystallinity from 69 to 73%, when the temperature of isothermal crystallization changes from 125°C to 137°C. Non-isothermally crystallized PP samples had lower crystallinity of 65%.

The main conclusion from data in Table 3 is that crystals are thicker and crystallinity is higher when the temperature of crystallization increases. The observed differences in lamellar thickness are result of the specific of applied DSC and SAXS methods. The different method applied for thickness measurements were compared some years ago by Zhou and Wilkes [26]. Previously, I studied properties of the same polymer, but prepared with a different cooling procedure during crystallization [15]. The comparison of results showed that if the PP film was slowly cooled from melt then its melting temperature was 163.1°C and heat of melting 90.9 J/g. If the same material was quickly cooled in water, the melting temperature decreased to 162.2°C and heat of melting was only 82.0 J/g. In both cases the process of solidification was faster than for the samples discussed in this manuscript.

Figure 2 shows exemplary images of 20 μm thick polypropylene slices observed with the

polarized light microscope. These slices represent cross-sections of non-deformed PP films. The supermolecular structure, with large spherulites is clearly visible on all photographs. Some of the spherulites were nucleated on the film surfaces (at the bottom of Fig. 2a or Fig. 2c), where the local temperature during cooling from T=220°C to crystallization temperature was lower than in the volume of specimen. This promoted the nucleation of spherulites on the surface. The nucleation was a little bit more frequent in the samples crystallized at higher temperatures (Fig. 2c), however not so intensive to dominate the structure formation. The spherulites were bigger in the samples crystallized isothermally, but the increase of size with temperature was moderate. In the samples crystallized isothermally, where the time of crystallization was longer, the formation of weak spots was observed, with breaking of structure in the largest of them. The exemplary weak spot is visible in the lower part of Fig. 2b. The elongated void, formed along the spherulites borders, is shown in Fig. 2d.

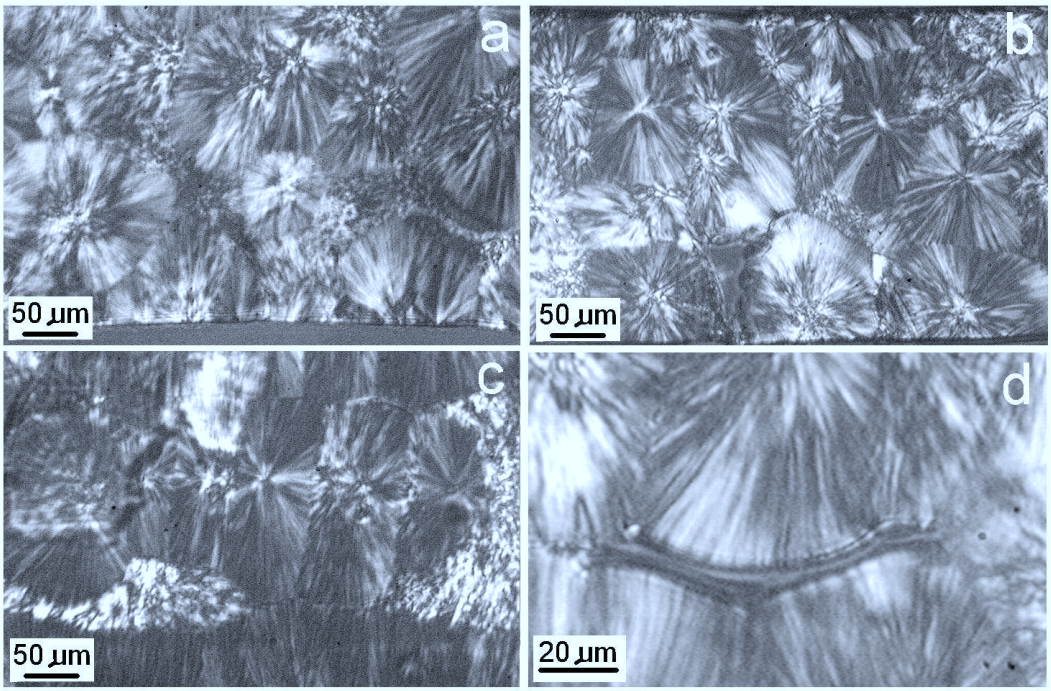


Fig. 2 The morphologies of polypropylene samples crystallized: non-isothermally (a), isothermally at 125°C (b), isothermally at 133°C (c) and a fragment of the structure of sample PP125, with a long void visible on the spherulitic border (d)

Results of the tensile test of PP samples are shown in Table 4 and representative stress-strain curves are presented in Fig. 3. The samples crystallized non-isothermally and at lower crystallization temperatures of 125 and 129°C were able to deform plastically with yield, however the structure broke shortly after the yield. The specimens crystallized at higher temperatures broke before the yield point. Elongation to break decreased with an increase of crystallization temperature and for the samples crystallized at 137°C it was only 1.5%. Samples crystallized at the temperatures of 133 and 137°C broke before the yield point. The elastic modulus, calculated from the stress at 1% of strain, increased slowly with the crystallization temperature. The mechanical properties of examined samples were not satisfactory for many applications, but the deterioration of some mechanical properties in more crystalline material is a well known phenomenon, observed for isothermally crystallized PP also by Pang et al. [16].

Table 4. Mechanical properties of PP samples deformed in tension at the rate of 2%/min.

Crystallization conditions [°C]	Elastic modulus [GPa]	Yield stress [MPa]	Yield strain [%]	Stress at break [MPa]	Strain at break [%]
Non-isothermal	1.3	31	9	29	13
125	1.2	32	8	30	12
129	1.3	32	7	30	8
133	1.3	-	-	27	6
137	1.4	-	-	9	2

Simultaneously with results of the mechanical test, small angle X-ray scattering patterns were recorded. The goal of these observations was to detect cavities. Figure 3 shows the stress-strain curves measured for individual samples and accompanying X-ray patterns recorded *in situ* during tensile drawing. The samples with maximum available strains were examined here with the aim of

getting maximum information on scattering and cavitation, so the strains to break on curves in Fig. 3 differ from the average values given in Table 4.

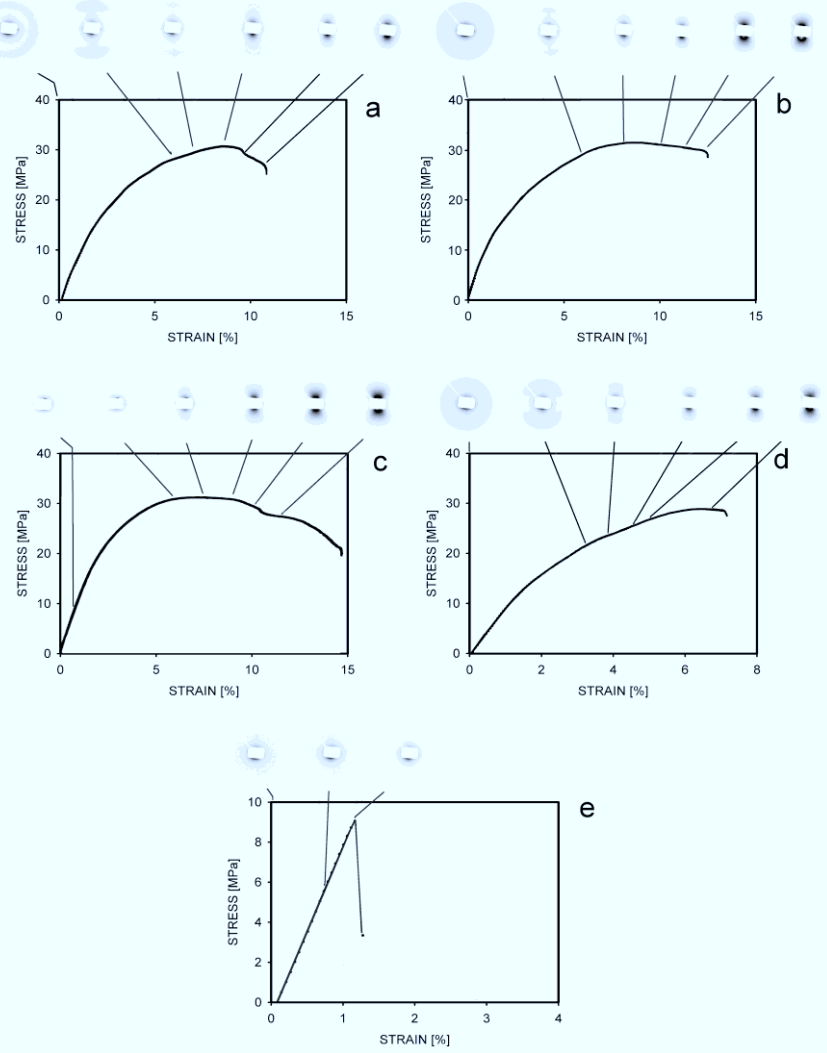


Fig. 3 SAXS patterns and stress-strain curves for polypropylene samples crystallized in the following conditions: a) non isothermal, b) 125°C, c) 129°C, d) 133°C, e) 137°C. The strains for which the patterns were registered are indicated by lines. The deformation direction on patterns was vertical

In the patterns representing non-deformed polypropylene only the scattering from periodic crystalline structure is visible. It is the evidence of an important fact that nano-voids are not formed in PP during isothermal crystallization. The very small black dots visible near the beam stop are traces of the non completely covered initial beam. In some images representing the deformed samples dark spots representing the scattering on cavities are visible. The first voids arise when the deformation is close to the yield. It happens for the samples crystallized non-isothermally and for samples crystallized isothermally at 125 and 129°C. Polypropylenes which were crystallized at higher temperatures cavitated earlier, before the yield point (see Fig. 3 d, e). It follows from Fig. 3e that first voids in the PP 137 specimen were formed at strain of 1.3% only. The vertical orientation of dark spots in scattering images is the evidence that the nano-size voids were elongated horizontally, i.e. perpendicularly to the deformation direction which was vertical.

From the patterns in Fig. 3 it is difficult to determine exactly the beginning of cavitation. For this goal it may be useful to analyse maximal intensities in scattering images as a function of deformation. These intensities should quickly increase from the moment when first nano-cavities are formed. Figure 4 presents relations between strain and maximal intensities visible on patterns in Fig. 3. A significant increase of intensity (more than 10%) was observed for non-isothermal PP-N sample when the strain reached 6.5%. In the samples crystallized isothermally such increase was noticed earlier: at 4% for PP 125 and PP 129 specimens, 3% for PP 133 and only 1.3% for PP 137. In each case the rise of intensity happened before the yield point. It means that cavitation preceded a large-scale plastic deformation of crystals occurring at yield. Especially the polypropylenes crystallized at the temperatures of 133 and 137°C cavitated very early. The curve representing PP 129 is not precisely in the middle between the curves for PP 133 and PP 125. A possible explanation is that for the PP 129 sample X-ray beam was not located exactly in the position where the cavitation was initiated first. The voids in beam position were formed here a moment later, with a time shift, which is seen in Fig. 4 as an increase of intensity at larger strain.

There is no general method for the determination of voids size directly from SAXS results;

however this size may be characterized by calculation of gyration radius, R, done according to Eq. 4. I analyzed vertical profiles of intensities from the scattering patterns, registered at the yield point. The background of scattering, resulting from the crystalline periodic structure, was subtracted,

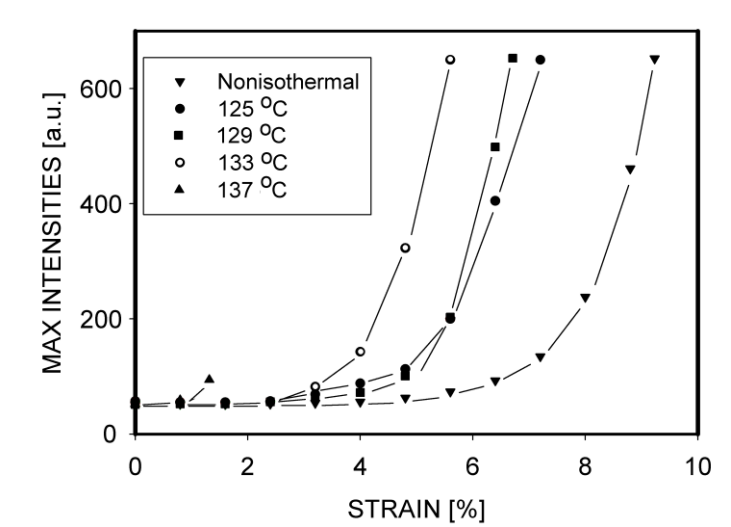


Fig. 4 Maximal intensities in SAXS patterns of deformed PP samples

assuming its shape similar to the one for the non-deformed sample. The procedure of determination of gyration radius from Eq. 4 is illustrated in Figure 5 on the example of non-isothermally crystallized PP sample. The following values of R were found: 30 nm for the non-isothermal sample, 28 nm for PP 125, 42 nm for PP 129 and 34 nm for PP 133. It means that systematic changes of gyration radius with crystallization conditions were not found. The sample PP 137 was broken much before the yield, however some limited cavitation was observed inside it, characterized by 50 nm radius of gyration.

The uniformity of deformation and shape of polypropylene samples are retained to the yield point. Beyond it the deformation concentrates in a small volume where a neck is formed. Because of this localization the changes of local dimensions are largest in the neck, where the local strain exceeds the macroscopic strains. These facts are illustrated in Fig. 6, where dimensions of the

sample, represented by local strain $(L-L_o)/L_o$ and width $(W-W_o)/W_o$ are shown as a function of engineering strain. They were determined in the position where the neck was formed. The distance between marks drawn on the surface of sample (i.e. 1 mm) was a basis for local strain

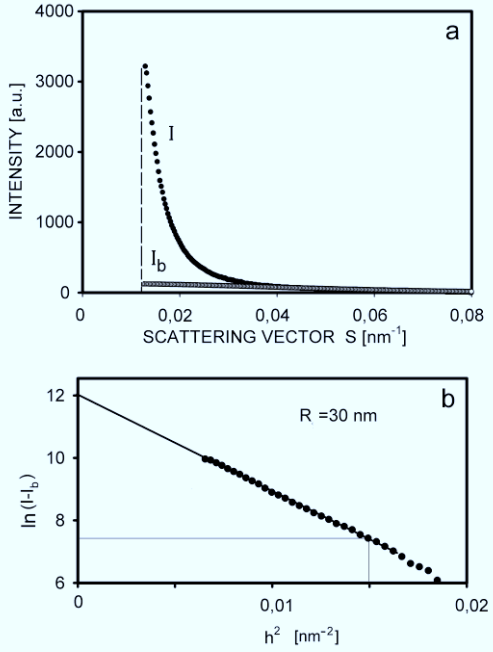


Fig. 5 a) Profiles of intensities measured in vertical direction in SAXS patterns shown in Fig 3a, representing the non-isothermal PP sample before deformation, I_b, and after deformation to yield strain, I. b) Logarithmic dependence of the scattering intensity $I-I_b$ as a function of square of the h vector ($h=2\pi s$). This dependence was used for determination of gyration radius R

determination. This particular sample, presented in Fig. 6, was crystallized at 129°C and its deformation to break was larger than typical for this kind of material (i.e. strain of 8%, see Table 4). A continuous declination of local strain data from straight line since the beginning of yield (i.e. 6% of strain) is clearly visible. The increase of length is accompanied by a decrease of the sample width. If the decrease is not proportional to the length increase, local volume of the sample changes. For the PP 129 specimen the increase of volume was observed for all strains.

The increase of volume before the yield is usually attributed to elastic deformation. In many case this increase is small and the accurate measurements of volume are difficult. A much larger increase of volume is often observed during the plastic deformation phase. Cavities formed inside the amorphous phase are responsible for it. Fortunately, for PP129 sample it was possible to

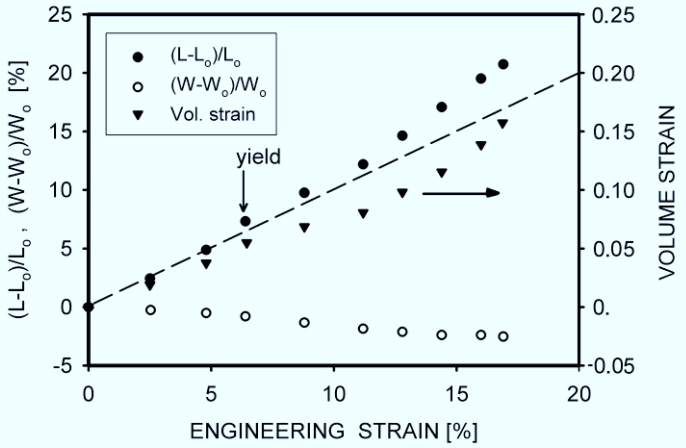


Fig. 6 Local strain $(L-L_o)/L_o$ and width $(W-W_o)/W_o$ in percent vs. engineering strain, measured in the most deformed part of PP129 sample. L is the actual and L_o the initial length between marks, W and W_o are the actual and initial width in the neck area. The dashed oblique line shows where the local strain is equal to engineering strain

measure correctly its dimensions up to the moment of break at 17% of strain. I found that the two-dimensional (i.e. defined as: length*width^2) volume strain at this deformation was equal to 0.16. It was more than the value of 0.1 determined previously for specimens of the same material, which were formed from the air-cooled melt [13]. The other PP specimens, crystallized in different conditions, broke around the yield and the experimental error of measurements was too large to determine the volume correctly.

b) Polyethylene

The second examined polymer was high-density polyethylene. Initial properties of HDPE

are presented in Table 5 which shows the data of long period and lamellae thickness, all determined in SAXS measurements. The long periods for isothermally crystallized specimens were larger than for these crystallized in non-isothermal conditions. Also the lamellae were thicker in isothermally crystallized samples (24.4 nm), when compared with the non-isothermal PE-N (19.9 nm).

The crystalline properties of HDPE have been also studied by using the DSC technique and results of measurements are shown in Table 5. This table shows a small increase of the melting temperature, heat of melting and crystallinity, when comparing PE-N with PE122 and PE125. Bassett showed that polyethylene lamellae are planar when the crystallization temperatures is higher than 127 ^{o}C [27]. Lower crystallization temperature produce spherulites whose lamellae have C or S-shaped profiles, in which the angle between lamellar normal and c axis changes continuously but with maximum ~35^{o} [27,28]. The values of lamellae thickness measured by SAXS were slightly different than those calculated from DSC data, which resulted from the specifics of both methods, however the general tendency - increase of thickness with temperature of crystallization- was preserved.

Table 5. Properties of non-deformed HDPE samples determined by the SAXS and DSC methods.

Temperature of crystalli-zation [°C]	SAXS			DSC			
	Long period (Is^2 vs. s) [nm]	Long period from correlation function [nm]	Lamellae thickness from correlation function [nm]	Temperature of maximum of melting peak [°C]	Lamellae thickness from Eq. 1 [nm]	Heat of melting [J/g]	Crystallinity* [%]
Non isothermal	31.4	27.8	19.9	135.9	21.9	236.9	82
122	34.6	30.8	23.8	136.7	25.3	240.0	83
125	33.3	32.1	24.4	136.9	26.3	243.7	84

*assuming the heat of fusion 289 J/g [29].

From the data in Table 5 and from previous observations [30, 31] I expected that cavitation

would appear in the samples crystallized isothermally and probably in the non-isothermal ones too. When the same polyethylene was solidified in air it had 21.1 nm thick lamellae and cavitated during stretching. However, if the molten HDPE samples were cooled in cold water then thinner lamellae grew (13.9 nm) and the polymer did not cavitate [30].

Similarly to polypropylene, the evolution of morphology during crystallization was observed in polyethylene by a polarized light microscope. The spherulitic structures were formed in all HDPE samples crystallized from melt. Spherulites were fine, with the diameter of a few micrometers only, so details of the structure were difficult to observe. The cavitation during crystallization was not visible.

The mechanical properties of polyethylene samples were tested during tensile drawing and the results are shown in Table 6 and in Figure 7. I found that the elastic modulus of isothermally crystallized specimens was by 12-14% larger than the modulus of PE-N. All samples were able to deform beyond the yield point. The values of yield stress were similar for the examined specimens, in the range of 27.0-27.4 MPa. Analysis of the yield strains showed that yield was reached earlier in the samples with larger crystals (i.e. PE 125 and PE 122). Elongations to break were not determined because mechanical tests were stopped after reaching plateau on the stress-strain curve, i.e. at the engineering strain of 90-120%, which was much before the break point of the examined materials (>400%).

Table 6. Mechanical properties of polyethylenes.

Crystallization conditions [°C]	Elastic modulus [GPa]	Yield stress [MPa]	Yield strain [%]
Non-isothermal	0.84	27.0	13.3
122	0.96	27.4	12.5
125	0.94	27.3	11.6

Part of the HDPE specimens were tensile tested with a simultaneous registration of scattered X-ray radiation. Examples of the stress-strain curves and related scattering patterns are shown in Fig. 7. The deformation of HDPE was non uniform and the neck was formed in all samples. Local strains in the neck were larger than macroscopic engineering strains. It is illustrated in Fig. 7, where the numbers near the curves show the values of local strain. Like polypropylene, the SAXS patterns for non-deformed samples contain only contribution from scattering on the crystalline periodic structure. It means that cavities with the size of 2-80 nm were absent in isothermally crystallized HDPE specimens before deformation. The intensive scattering on cavities is clearly visible in deformed samples. It is first observed shortly before the yield, at strains of 11-12%.

The patterns recorded beyond the yield are oriented in the deformation direction (i.e. vertically in Fig. 7), which means that cavities were elongated perpendicularly to the deformation direction. At some local strain, in the range of 100-200 % the shape of pattern changes. This is interpreted as a reorientation of voids into the deformation direction. From the evolution of patterns it may be deduced that voids were more elongated at higher strains. The changes of void shapes were similar to those observed previously for HDPE [30, 31], when the samples were slowly solidified in air or were annealed.

The X-ray scattering on voids was most intensive for the PE 125 sample, however the differences in intensities between specimens are difficult to estimate from Fig. 7. It will be helpful to analyze scattering profiles. Figure 8 presents intensity profiles taken in the deformation direction for samples deformed to 25% of the engineering strain, i.e. shortly after the beginning of cavitation. It is clear that the most intensive scattering was from the PE 125 sample and the lowest intensities were measured for the PE-N specimen.

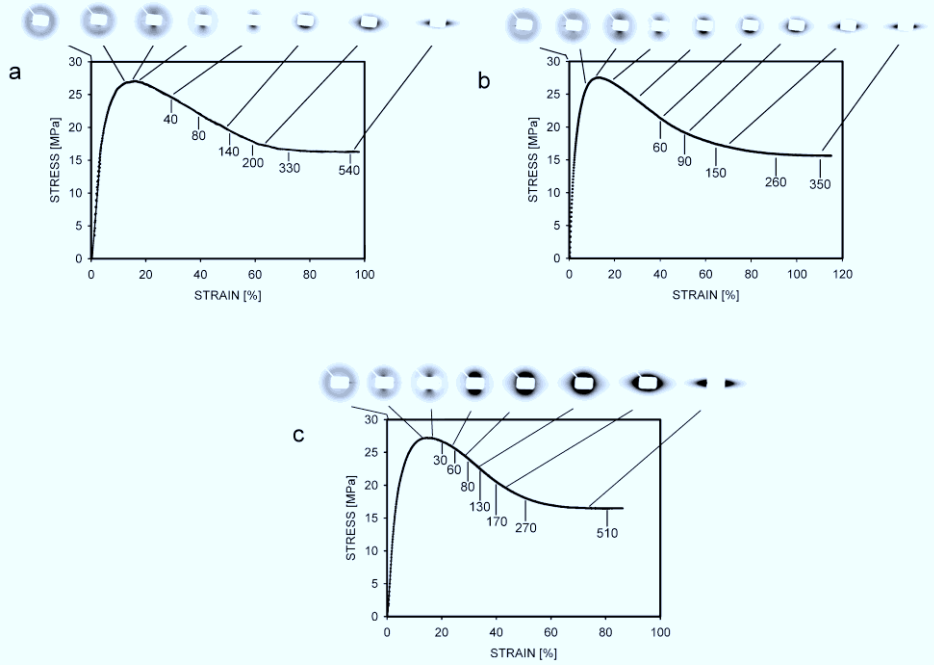


Fig. 7 Stress-strain curves and SAXS patterns registered at selected strains for HDPE samples: a) non-isothermally crystallized, b) crystallized at the temperature of 122°C, c) crystallized at the temperature of 125°C. The numbers show local strains in percent. The deformation direction on patterns is vertical

Additionally to profiles in Fig. 8, total scatterings from the samples, registered by a Mar CCD detector, were determined. Darkening of the scattering pattern was analyzed using the Image J 1.41 software (public domain, author: W. Rasband, National Institute of Mental Health, USA). It was done for specimens deformed to engineering strains of 25%, i.e. when the cavitation was relatively intensive, but the local strains in the samples were comparable. The performed analysis showed that if scattering from the non-isothermally crystallized sample was normalized to 1.0, then for PE 122 it was 1.18 and for PE 125 it was 1.42. These results confirm that at the beginning of plastic deformation the scale of cavitation strongly depends on the previous crystallization process.

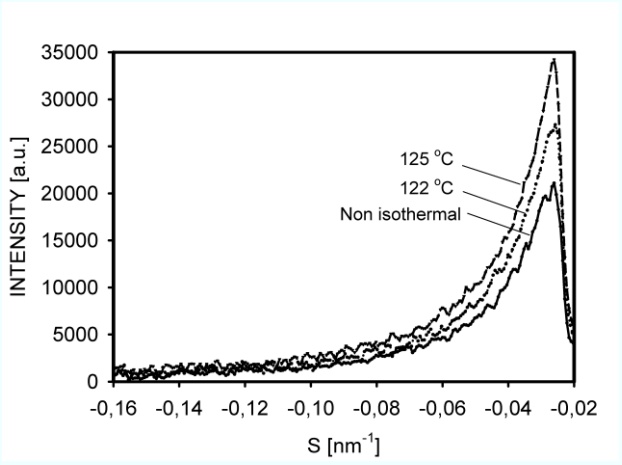


Fig. 8 Scattering profiles taken in the vertical direction from patterns in Fig. 7, representing samples deformed to engineering strain of 25%. The decreasing intensity on the right side indicates the edge of the beam stop. S is the scattering vector

An important aspect of the cavitation process is the size of cavities, because together with the number of voids it affects the behaviour and properties of material. It is known that the intensity of scattering is proportional to the square of total volume of scattering objects. Guinier's approach (eq. 4) may be used to calculate size if the voids are dispersed in the polymer [25], which happens at the beginning of cavitation. Computations of the radius of gyration were carried out for samples deformed to 20% of the engineering strain. Here the vertical profiles of intensities were analyzed, taken from scattering patterns in Fig. 7. Because the scattering from voids dominated, it was assumed that the background and scattering from crystalline structures was on the same level as the scattering from non-deformed polymer and both were subtracted from the total scattering. The calculations showed that only one population of nano voids existed in the HDPE samples. The radius of gyration was equal to 14.8 nm for non-isothermally crystallized HDPE, 16.7 nm for the same polymer crystallized at 122°C and 16.5 nm for the HDPE sample crystallized at 125°C.

Cavitation is the process in which a new volume is created. Thus, the measurement of volume increase is the way to characterize the scale of cavitation. Changes of the volume strain (defined by Eq. 3) as a function of the local strain are shown in Fig. 9. The presented dependences were

registered for individual samples and represented a typical behaviour for particular crystallization temperatures. However, it should be mentioned that data for the individual samples within the set may be a little different than typical, because the volume increase is sensitive to the degree of localization of deformations in the neck and the neck shape was not exactly the same for the compared samples. The samples in which the neck was well developed immediately after the yield had a larger volume strain than the samples where the neck formation was a longer process.

A significant increase of volume was observed in all samples, beginning from the yield point. The volume strain was similar for the PE-N and PE 122 specimens, but a much stronger increase was observed for PE 125, where the volume of the analyzed element was even twice as big as the original one.

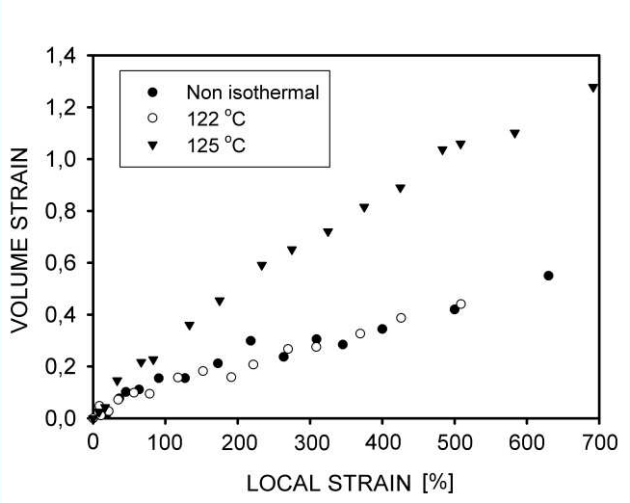


Fig. 9 Dependence of volume strain $((V-V_o)/V_o)$ on the local strain for polyethylene samples

It is known that not only nano-voids, but also micrometer-size voids are responsible for the volume increase. Voids of this size scatter light, and when the material is observed in reflected light it is whiter than the initial one. The presence of micrometer-size voids in examined PE was confirmed by whitening which occurred at yield. I excluded from the consideration the second potential reason of whitening, i.e. additional crystallization of strained polymer – because the DSC studies did not show an increase of crystallinity for the deformed polymer. WAXS observations

showed the changes in crystalline polymorphs with deformation. Two-dimensional patterns were registered for non-deformed samples (Fig. 10 a), for the same sample deformed to yield (Fig. 10 b) and after stress release (Fig. 10 c). Two circles, which showed up in the WAXS patterns for undeformed material and for strained to yield, are associated with a diffraction from (110) (inner circle) and (200) (outer circle) lattice planes of orthorombic form. In the samples under preserved strain at yield a third ring, inside the (110) ring, appears visible, indexed as (001) of monoclinic form. This form is a result of martensitic transformation of orthorhombic form under stress. The monoclinic form is not visible in the pattern at such strain if the sample was relaxed with free ends. The reversibility of transition is not accompanied by similar effect of whitening, which exclude crystallographic changes from the factors responsible for whitening.

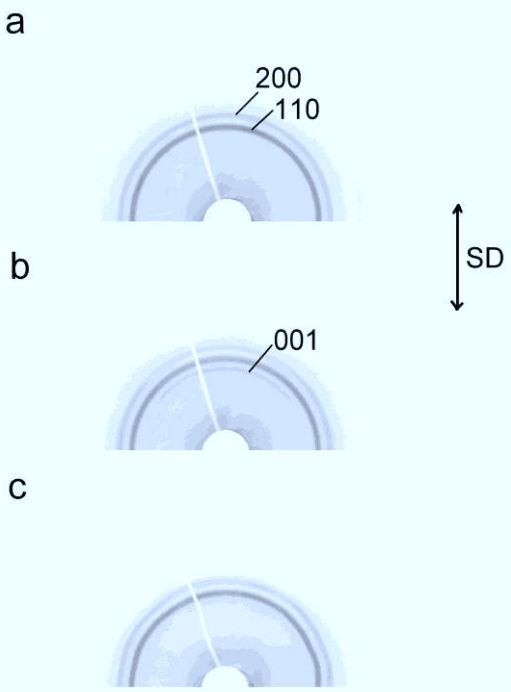


Fig. 10 WAXS patterns registered for PE122 sample before deformation (a), after deformation to yield point (b), and after deformation to yield and release of stresses with free ends (c). The main diffracting crystallographic planes are indicated. SD is the direction of deformation

The example of whitening effect for the deformed sample is presented in Figure 11a. It is the PE-N specimen observed in transmitted light after deformation. The source of light was the Image Eraser, produced by Molecular Dynamics, usually used for erasing of imaging plates. This equipment gives uniform white light on a large surface. The objects of investigations were polyethylene samples deformed to plateau on the stress-strain curve, with similar length of the neck and with similar thickness after deformation, in the range of 0.29±0.01 mm measured in the central part of neck. The samples were placed on the transparent plate and photographed. Intensive scattering of the transmitted light in the neck part of the specimen is visible in the photographs as a dark area. In reflection mode the same area is seen as being whiter. The observations showed that the scale of light scattering depended on the sample. Figure 11b shows profiles of intensities taken

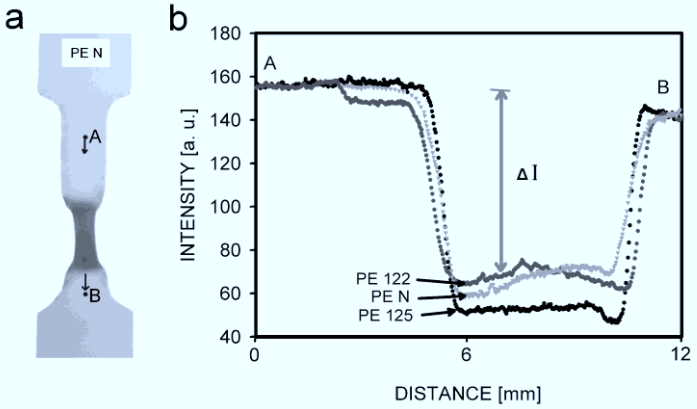


Fig. 11 PE-N sample illuminated by light going through the sample (a) and intensity of light transmitted through the sample, measured along the line between points A and B for PE-N, PE 122 and PE 125 (b)

from point A to point B for the PE-N sample (see Fig. 11a) and by the same way for the rest of my specimens. The most intensive scattering in the neck was for the PE 125 sample. Scattering for two other samples was on a similar level. If the mean values of grey levels on the photographs

determined for neck area using the Image J software are compared, the relations of intensity decreases, ΔI, are 1.0 : 1.02 : 1.12 for PE 122, PE-N and PE 125, respectively. This is in good agreement with measurements of the volume in Fig. 9, where similarities for PE-N and PE 122 were visible, but the volume for PE 125 was much bigger. The results of volume strain and light and X-ray scatterings show that nano- and micro-voids are most intensive in PE 125. In the PE 122 sample the nano-voids are more frequent than in PE-N, however the volume increase is similar for PE 122 and PE-N, which means that microvoids are more frequent in PE-N or the frequencies are similar, but the contribution from microvoids dominates in the volume strain.

CONCLUSIONS

The experiments performed with two polymers – polypropylene and high-density polyethylene – showed that plastic deformation of these materials occurs with cavitation. Their mechanical properties and process of cavitation depend on the conditions at which the polymer was crystallized. Although both polymers were crystallized isothermally their morphologies were different. In polyethylene small, a few micrometers in diameter spherulites grew, so also small weak-spots were formed between them and micrometer size cavities were not formed during crystallization [5]. The SAXS studies showed that nano voids were not present in non-deformed HDPE. The cavitation happened when the external force was applied to HDPE specimen. Voids were observed for the first time before the yield point, at strains of 1-2% below the yield strain.

The DSC and SAXS measurements confirmed that crystallinity and crystal thickness of polyethylene increased with temperature and time available for crystallization. It is known that higher crystallinity and thicker, less defected crystals favour the cavitation during deformation [10]. These resulted in the most intensive cavitation (both nano and micrometer size) observed in polyethylene samples crystallized at the highest temperature. The nanovoids were at yield elongated perpendicularly to the deformation direction, which indicates that they were formed between the

lamellae inside spherulites, not on the spherulitic borders or not inside the weak spots. Inside the spots and on the borders more random orientation and less elongated voids are expected. Moreover, some observations of the isothermally crystallized samples showed that melting inside weak spots occurred at lower temperatures than melting of surrounding spherulites, which means that the mater inside these spots is less organized, with more defected crystals. The conditions for cavitation inside weak spots are worse than these existing inside the spherulities.

The elongated shapes of SAXS patterns mean that the radius of gyration, R, is not directly related to the real dimension of voids and depends on the measurement direction. In current studies the radius of gyration in vertical direction was 15-17 nm.

Evolution of the shape of nano cavities with elongation was similar in all samples and resembled those studied previously [31]. The voids were initially elongated perpendicularly to the deformation direction, but this orientation changed for large strains, where cavities were elongated in the deformation direction. The change was forced by the reorganization of surrounding lamellae, just as it was described in previous papers [13,14,30,31]. The small voids were accompanied by larger, micrometer size. Their presence was confirmed by whitening of material which occurred after yield.

The internal structure of the second examined polymer, polypropylene, was different, because larger spherulites were grown during crystallization. Morphological observations showed that large weak spots, with the diameter of 10-100 μm, were formed between spherulites in the isothermally crystallized films. In some of them the polymer cavitated near the end of crystallization, forming micrometer size voids. SEM photographs showed that weak spots were not very frequent. Nowacki et al. [5] observed that the negative pressure build up was slower in large weak spots formed in polypropylene specimens crystallized at highest temperatures. The reason was some relaxation of stretched molecules possible during long crystallization and reduced viscosity of melt. This resulted in less frequent micro cavitation observed during crystallization in highest temperatures although the weak spots were larger. The SAXS studies showed that the large voids

in PP were not accompanied by smaller, nanometer-size voids.

The crystals in PP samples were thick, so it was supposed that tensile deformation would occur with cavitation, which was confirmed experimentally for all examined samples. When the polymer was deformed voids were observed for the first time before the yield point. In polypropylene the cavitation began earlier (i.e. at smaller strains) for these samples which were crystallized at higher temperatures. The DSC and SAXS measurements confirmed that crystallinity and crystal thickness of polypropylene increased with temperature and time available for crystallization. It is known that more regular chain folding in higher crystallization temperatures results in decreasing of the number of tie molecules [32]. These molecules connecting adjacent crystallities play important role in the mechanical performance of polymers [33,34]. Limited number of the molecules bridging lamellae cannot preserve the continuity of amorphous phase when the polymer is stretched. This is a possible reason of the early cavitation observed in these polypropylene specimens which were formed at highest temperatures.

The SAXS patterns confirmed that nano cavities in PP were elongated perpendicularly to the drawing direction. The intensities of scattering at yield, depending on the scale of cavitation, were larger for the specimens crystallized at higher temperatures. The volume strain for PP 129 sample was larger than these reported previously for the same polymer crystallized when cooling was in air [12,14,24].

Polypropylene spherulites usually are built from the lamellae of α crystallographic form, creating so-called cross-hatching structure. Previous studies of the cavitation in α and β allotropic modifications of PP showed that scale of voiding was larger in β form, where this structure is not present, but only the radial lamellae growth [14]. Norton and Keller [35] and Janimak et al. [36] found that cross-hatching density in isothermally crystallized PP is reduced with temperature and radial lamellae dominate at higher crystallization temperatures. So, the arrangement of lamellae crystallized at higher temperature resembles that characteristic for β form specimens and it should result in more intensive cavitation during deformation. This is a reason, aside decreasing number of

tie molecules, that the amorphous phase is weaker and more intensive cavitation is observed in the samples crystallized at higher temperatures.

The size of cavities was estimated from the radius of gyration. The samples which were crystallized in controlled isothermal conditions had bigger values of R (i.e. 28-50 nm) than those found previously for PP crystallized by another cooling procedure (13-18 nm). The larger values of R were not associated with the increase of amorphous layer thickness.

The above observations lead to the conclusion that cavitation is more intensive when the crystallinity is higher and crystals are thicker, which happens during isothermal crystallization at high temperatures. Comparison of the cavitation during deformation in polypropylene containing some micro voids resulting from crystallization and in polyethylene without such voids shows that nano voiding process occur similarly, i.e. without visible influence of pre existing micro voids. Those micro voids are present in the interspherulitic areas, separated from the interlamellar amorphous layers inside spherulites, where the new nano voids are generated during deformation. The large weak spots and big voids disturbing the internal distribution of stresses are probably responsible for poor tensile properties and early break of PP samples.

Acknowledgments:

I wish to express thanks to the Hamburg Synchrotron Radiation Laboratory for the beam time granted within the projects I 20100253 EC and I 20110505 EC. Also the statutory fund of the Centre of Molecular and Macromolecular Studies, Polish Academy of Sciences is acknowledged.

LITERATURE

1. Pawlak A, Galeski A (1990) Stability of Spherulite Growth. J Polym Sci B Polym Phys 28:1813-1821
2. Galeski A, Piorkowska E (1983) Localized Volume Deficiences as an Effect of Spherulite Growth. II. The Three-Dimensional Case. J Polym Sci Polym Phys Ed 21:1313-1322
3. Pawlak A, Piorkowska E (1999) Effect of Negative Pressure on Melting Behavior of Spherulites in Thin Films of Several Crystalline Polymers. J Appl Polym Sci 74:1380-1385.
4. Galeski A, Koenczoel L, Piorkowska E, Baer E (1987) Acoustic-Emission During polymer Crystallization. Nature 325 (6099): 40-41
5. Nowacki R, Kolasinska J, Piorkowska E (2001) Cavitation during isothermal crystallization of isotactic polypropylene. J Appl Polym Sci 79:2439-2448
6. Varga J, Ehrenstein GW (1996) Formation of beta-modification of isotactic polypropylene in its late stage of crystallization. Polymer 37:5959-5963
7. Monasse B, Haudin JM (1985) Growth transition and morphology change in polypropylene. Coll Polym Sci 263:822-831
8. Thomann R, Wang Ch, Kressler J, Mulhaupt R (1996) Negative pressure effects during the isothermal crystallization of isotactic poly(propylene) studied by light and atomic force microscopy. Macromol Chem Phys 197:1085-1091
9. Galeski A, Piorkowska E (1983) Localized Volume Deficiences as an Effect of Spherulite Growth. I. The Two-Dimensional Case. J Polym Sci Polym Phys Ed 21:1299-1312
10. Pawlak A, Galeski A (2005) Plastic Deformation of Crystalline Polymers:The Role of Cavitation and Crystal Plasticity. Macromolecules 38:9688-9697
11. Pawlak A, Galeski A (2011) Cavitation during tensile drawing of semicrystalline polymers. Polimery 56:627-636
12. Pawlak A, Galeski A (2008) Cavitation during Tensile Deformation of Polypropylene.

Macromolecules 41:2839-2851

13. Pawlak A, Galeski A (2010) Cavitation and Morphological Changes in Polypropylene Deformed at Elevated Temperatures. J Polym Sci Part B: Pol Phys 48:1271-1280
14. Pawlak A (2012) Cavitation during deformation of polymers on the example of polypropylene. J Appl Polym Sci 125:4177-4187
15. Pawlak A, Galeski A (2012) Thermovision Studies of Plastic Deformation and Cavitation in Polypropylene. Mech Mater (sent to editor)
16. Pang Y, Dong X, Liu K, Han CC, Chen E, Wang D (2008) Ductile-brittle transition controlled by isothermal crystallization of isotactic polypropylene and its blend with poly(ethylene-co-octene). Polymer 49:4259-4270
17. Kennedy MA, Peacock AJ, Mandelkern L (1994) Tensile Properties of Crystalline Polymers: Linear Polyethylene. Macromolecules 27:5297-5310
18. Hoffman JD (1982) Role of reptation in the rate of crystallization of polyethylene fractions from the melt. Polymer 23:656-670
19. Crist B (2007) Yet Another Visit to the Melting of Polyethylene Crystals. J Polym Sci Part B Polym Phys 45:3231-3236
20. Clark EJ, Hoffman JD (1984) Regime III crystallization in polypropylene. Macromolecules 17: 878-885
21. Galeski A (1997) Macromolecular Displacements and Entanglements of Flexible Chains in Polymers on Crystallization. Polimery 42:432-440
22. Stribeck N (2007) X-ray Scattering of Soft Matter. Springer-Verlag, Berlin Heidelberg, pp.117-118
23. Strobl GR, Schneider M (1980) Direct evaluation of the electron-density correlation-function of partially crystalline polymers. J Polym Sci Polym Phys Ed 18:1343-1359
24. Goderis B, Reynaers H, Koch MHJ, Mathot VBF (1999) Use of SAXS and linear correlation functions for the determination of the crystallinity and morphology of semi-crystalline

polymers. Application to linear polyethylene. J Polym Sci Part B Polym Phys 37:1715-1738

25. Guinier A (1963) X-Ray Diffraction In Crystals, Imperfect Crystals and Amorphous Bodies. W. H. Freeman and Company, San Francisco and London, pp 322-332
26. Zhou H, Wilkes GL (1997) Comparison of lamellar thickness and its distribution determined from d.s.c., SAXS, TEM and AFM for high-density polyethylene films having a stacked lamellar morphology. Polymer 38:5735-5747
27. Patel D, Basset DC (2002) On the formation of S-profiled lamellae in polyethylene and the genesis of banded spherulites. Polymer 43:3795-3802
28. Bassett DC (2004) Polymer morphology: A guide to macromolecular self-organization. Macromol Symp 214: 5-15
29. Quinn FA, Mandelkern L (1958) Thermodynamics of crystallization in high polymers-poly(ethylene). J Am Chem Soc 80:3178-3182
30. Pawlak A (2007) Cavitation during tensile deformation of high-density polyethylene. Polymer 48:1397-1409
31. Pawlak A, Galeski A (2010) Cavitation during tensile drawing of annealed high density polyethylene. Polymer 51:5771-5779
32. Li Y, Iwakura Y, Shimizu H (2008) Polymer Crystallites with few Tie Molecules from a Miscible Polymer Blend. Macromolecules 41:3396-3400
33. Seguela R (2005) Critical Review of the Molecular Topology of Semicrystalline Polymers: The Origin and Assessment of Intercrystalline Tie Molecules and Chain Entanglements. J Polym Sci Part B: Polym Phys 43:1729-1748
34. Henning S, Michler GH (2005) Micromechanical Deformation Mechanisms in Polyolefins: Influence of Polymorphism and Molecular Weight. In: Michler GH, Balta-Calleja FJ (eds) Mechanical Properties of Polymers Based on Nanostructure and Morphology. Taylor & Francis Group, Boca Raton, pp 245-278
35. Norton DR, Keller A (1985) The spherulitic and lamellar morphology of melt-crystallized

Sformatowano

isotactic polypropylene. Polymer 26:704-716

36. Janimak JJ, Cheng SZD, Giusti PA, Hsieh ET (1991) Isotacticity Effect on Crystallization and Melting in Poly(propylene) Fractions. Macromolecules 24:2253-2260

FIGURES:

Fig. 1 Heat flow as a function of time during isothermal crystallization of PP samples at selected temperatures: 125, 129, 133 and 137°C
Fig. 2 The morphologies of polypropylene samples crystallized: non-isothermally (a), isothermally at 125°C (b), isothermally at 133°C (c) and a fragment of the structure of sample PP125, with a long void visible on the spherulitic border (d)
Fig. 3 SAXS patterns and stress-strain curves for polypropylene samples crystallized in the following conditions: a) non isothermal, b) 125°C, c) 129°C, d) 133°C, e) 137°C. The strains for which the patterns were registered are indicated by lines. The deformation direction on patterns was vertical
Fig. 4 Maximal intensities in SAXS patterns of deformed PP samples
Fig. 5 a) Profiles of intensities measured in vertical direction in SAXS patterns shown in Fig 4, representing the non-isothermal PP sample before deformation, I_b, and after deformation to yield strain, I. b) Logarithmic dependence of the scattering intensity $I-I_b$ as a function of square of the h vector ($h=2\pi s$). This dependence was used for determination of gyration radius R.
Fig. 6 Local strain $(L-L_o)/L_o$ and width $(W-W_o)/W_o$ in per cent vs. engineering strain, measured in the most deformed part of PP129 sample. L is the actual and L_o the initial length between marks, W and W_o are the actual and initial width in the neck area. The dashed oblique line shows where the local strain is equal to engineering strain
Fig. 7 Stress-strain curves and SAXS patterns registered at selected strains for HDPE samples: a) non-isothermally crystallized, b) crystallized at the temperature of 122°C, c) crystallized at the temperature of 125°C. The numbers show local strains in per cent. The deformation direction on patterns is vertical
Fig. 8 Scattering profiles taken in the vertical direction from patterns in Fig. 7, representing samples deformed to engineering strain of 25%. The decreasing intensity on the right side indicates the edge of the beam stop. S is the scattering vector
Fig. 9 Dependence of volume strain $((V-V_o)/V_o)$ on the local strain for polyethylene samples
Fig. 10 WAXS patterns registered for PE122 sample before deformation (a), after deformation to yield point (b) and after deformation to yield and release of stresses with free ends (c). The main diffracting crystallographic planes are indicated. SD is the direction of deformation.
Fig. 11 PE-N sample illuminated by light going through the sample (a) and intensity of light transmitted through the sample, measured along the line between points A and B for PE-N, PE 122 and PE 125 (b)

TABLES

Table 1. Times of crystallization determined from DSC studies as appropriate for the crystallization of samples designed for mechanical studies.

Table 2. List of samples studied in mechanical and SAXS tests.

Table 3. Results of SAXS and DSC experiments for non-deformed PP samples.

Table 4. Mechanical properties of PP samples deformed in tension at the rate of 2%/min.

Table 5. Properties of non-deformed HDPE samples determined by the SAXS and DSC methods.

Table 6. Mechanical properties of polyethylenes.